Journal of Engineering Physics and Thermophysics, Vol. 79, No. 3, 2006

HYDROGASDYNAMICS IN TECHNOLOGICAL PROCESSES

INFLUENCE OF THE GEOMETRY OF THE NOZZLE ON THE CHARACTERISTICS OF AN EXHAUST JET

O. G. Buzykin, M. N. Kogan, and A. N. Kucherov

UDC 533.6+532.517

Two solutions for the parameters of a turbulent exhaust jet of a dual-duct engine — the traditional solution within the framework of Prandtl equations of the type of boundary-layer equations and calculation of the near-range field within the framework of the Navier–Stokes equations with subsequent calculation within the framework of the Prandtl equations for large distances — have been compared. It has been shown that the influence of the real geometry of the nozzle exit section, including the shift of the center body and the main duct forward from the exit section of the cold secondary duct, can be allowed for by correcting the constant of the source term in the differential equation for turbulent kinematic viscosity.

Introduction. In calculating the turbulent jet from the exhaust nozzle of an engine [1], one usually assumes that the nozzle exit section is planar and the transverse distributions of the parameters (temperature, velocity, etc.) are uniform. In the case of a nonisobaric jet in a wide range of the nonisobaricity parameter — a ratio of the pressure on the nozzle exit section to the pressure in the surrounding space of 0.5 to 2.0 — the initial parameters of the jet ρ_e, u_e, r_e, and T_e in the cross section of equalization of the pressure $p_e(x_e) \approx p_\infty$ can be calculated from the formulas of adiabatic (H = const) and isentropic (p/ρ^γ = const) expansion [2–5]. The rear part of the exhaust nozzle of a dual-duct engine [6] has the main duct A′H shifted forward from the section of the nozzle of the secondary duct A′B′ and the center body GF shifted forward from the main-duct-nozzle section (Fig. 1). In this case, too, we can specify the initial conditions in the pressure-equalization cross section within the framework of a quasi-one-dimensional approximation; the parameters ρ_e, u_e, r_e, and T_e can be calculated from the integrals of conservation of the mixture mass and the vapor mass and the total enthalpy and entropy. When the nonisobaricity in the pressure-equalization cross section is low, it is the transverse dimensions of the tubes of current of the main and secondary ducts that change first. The characteristics of the jet, including the long-range field, are affected by these changes only slightly. When the slopes of the elements shifted forward are considerable, the assumption of quasi-one-dimensionality is disturbed. Furthermore, the condition of sticking of a gas on solid surfaces and disturbances in turbulent boundary layers introduce additional disturbances into the non-one-dimensional pattern of flow. It becomes necessary to calculate the long-range field using Navier–Stokes elliptic equations with allowance for the second derivatives with respect to the longitudinal coordinate. The consumption of computer time substantially increases. In this case, too, the long-range field can be calculated using just Prandtl parabolic equations in which the second derivatives along the axial coordinate are disregarded. This brings up the questions of agreement of the turbulence models, length of the Navier–Stokes domain, applicability of the traditional assignment of the initial parameters in the pressure-equalization cross section, and legitimacy of direct calculation of the jet using Prandtl equations. The present work seeks to show that the traditional approach (with certain corrections) is also true for the case of a substantial influence of the geometry of the rear part of the exhaust nozzle.

N. E. Zhukovskii Central Aerohydrodynamic Institute, Zhukovskii-3, 140180, Moscow Region, Russia. Translated from Inzhenerno-Fizicheskii Zhurnal, Vol. 79, No. 3, pp. 37–46, May–June, 2006. Original article submitted September 9, 2004; revision submitted March 22, 2005.

1062-0125/06/7903-0456

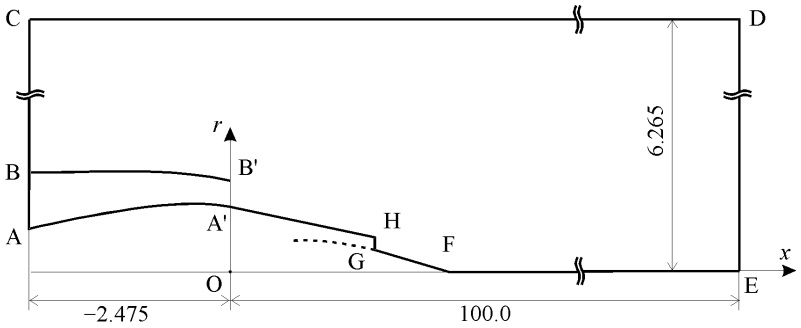

Fig. 1. Geometric scheme of the protruding part of the exhaust nozzle of a dual-duct engine ABB′A′HGF and the computational domain within the framework of Navier–Stokes ACDE (r = 0–6.265 m and x = −2.475 to 100 m).

Formulation of the Problem within the Framework of the Navier–Stokes Equations (Reynolds equations for the average parameters of turbulent flow [7]). In the vicinity of the nozzle exit section, the second derivatives of the functions sought with respect to the longitudinal coordinate are quantities of the same order as the remaining terms of the mass, momentum, and energy equations. We solved the problem on stationary, axisymmetric, slightly off-design (nonisobaric) flow of a compressible gas out of two coaxial annular nozzles into the cocurrent flow. Air flows through the external nozzle, whereas air with an admixture of steam flows through the internal nozzle. The flow was described by Reynolds-averaged Navier–Stokes equations [8]:

$$\frac{\partial \rho}{\partial t} + \frac{\partial}{\partial x_j}(\rho u_j) = 0 , \tag{1}$$

$$\frac{\partial}{\partial x_j}(\rho u_j u_i - \tau_{ij}) = -\frac{\partial p}{\partial x_i} , \tag{2}$$

$$\frac{\partial}{\partial x_j}(\rho u_j H - q_j - u_i \tau_{ij}) = 0 , \tag{3}$$

$$\frac{\partial}{\partial x_j}(\rho u_j Y - j_j) = 0 . \tag{4}$$

Here

$$\tau_{ij} = 2\mu s_{ij} - \frac{2}{3}\mu \frac{\partial u_k}{\partial x_k}\delta_{ij} - \rho \overline{u_i' u_j'} \tag{5}$$

are the components of the stress tensor;

$$s_{ij} = \frac{1}{2}\left(\frac{\partial u_i}{\partial x_j} + \frac{\partial u_j}{\partial x_i}\right) \tag{6}$$

are the components of the strain-rate tensor;

$$H = \frac{1}{2} u_i u_i + C_p T$$

is the total enthalpy;

$$q_j = \lambda \frac{\partial T}{\partial x_j} - \rho C_p \overline{u_j' T'} \tag{7}$$

are the components of the heat-flux vector;

$$j_j = \rho D \frac{\partial Y}{\partial x_j} - \rho \overline{u_j' Y'} \tag{8}$$

are the components of the diffusion-vapor-flow vector.

Summation over the double subscripts is implied in the equations; when the subscripts coincide, the quantity δ_{ij} is equal to 1; in other cases it is equal to zero. The pulsation components of the corresponding quantities are primed; the bar denotes averaging. The Reynolds stresses and fluxes are computed from the formulas

$$\rho \overline{u_i' u_j'} = -2\mu_t s_{ij} + \frac{2}{3}\left(\mu_t \frac{\partial u_k}{\partial x_k} + \rho k\right)\delta_{ij}, \tag{9}$$

$$\rho \overline{u_j' T'} = -\frac{\mu_t}{\mathrm{Pr_t}} \frac{\partial T}{\partial x_j}, \tag{10}$$

$$\rho \overline{u_j' Y'} = -\frac{\mu_t}{\mathrm{Sc_t}} \frac{\partial Y}{\partial x_j}, \tag{11}$$

where $\mathrm{Pr_t}$ and $\mathrm{Sc_t}$ are respectively the turbulent Prandtl and Schmidt numbers representing empirical constants ($\mathrm{Pr_t}$ = $\mathrm{Sc_t}$ = 0.9) and μ_t is the turbulent-viscosity coefficients related to the turbulent parameters using the k–ε model:

$$\mu_t = C_\mu \frac{\rho k^2}{\varepsilon}. \tag{12}$$

Here C_μ = 0.085 is the empirical constant. We use the following transfer equations for the turbulence parameters:

$$\frac{\partial}{\partial x_j}\left(\rho u_j k - \frac{\mu + \mu_t}{\sigma_k}\frac{\partial k}{\partial x_j}\right) = 2\mu_t s_{ij}\frac{\partial u_i}{\partial x_j} - \frac{2}{3}\left(\mu_t \frac{\partial u_i}{\partial x_i} + \rho k\right)\frac{\partial u_i}{\partial x_i} - \rho\varepsilon, \tag{13}$$

$$\frac{\partial}{\partial x_j}\left(\rho u_j \varepsilon - \frac{\mu + \mu_t}{\sigma_\varepsilon}\frac{\partial \varepsilon}{\partial x_j}\right) = 1.42\frac{\varepsilon}{k}\left[2\mu_t s_{ij}\frac{\partial u_i}{\partial x_j} - \frac{2}{3}\left(\mu_t \frac{\partial u_i}{\partial x_i} + \rho k\right)\frac{\partial u_i}{\partial x_i}\right] -$$

$$- 1.68\rho\frac{\varepsilon^2}{k} - 0.378\rho\varepsilon\frac{\partial u_i}{\partial x_i} - C_\mu \frac{\eta^3(1 - 0.228\eta)}{1 + 0.012\eta^3}\frac{\rho\varepsilon^2}{k}, \tag{14}$$

$$\eta = \frac{k}{\varepsilon}\sqrt{2\overline{s_{ij}s_{ij}}}; \quad \sigma_k = \sigma_\varepsilon = 0.719.$$

To exemplify calculation we take the following specific parameters of the engine's exhaust nozzle. The geometry of the exhaust nozzle of a dual-duct engine is diagrammatically presented in Fig. 1. The x axis is guided along the jet, whereas the r axis is guided across it. The center body on the axis is shifted from the exit section of the main-duct nozzle by the distance l_1 = 0.93 m, and the main duct is shifted forward from the exit section of the nozzle of a cold secondary duct by the distance l_2 = 1.82 m. Point B′ corresponds to the coordinates (x = 0, r_2 = 1,147 m),

point A′ corresponds to (0, r_{20} = 0.822 m), point H corresponds to ($x = l_2$, r_1 = 0.435 m), and point G corresponds to (l_2, r_{10} = 0.279 m).

We take that the pressure in the outer atmosphere at a cruising altitude of 11 km is p_∞ = 22,690 N/m^2, the temperature is T_∞ = 216.7 K (air density ρ_∞ = 0.36523 kg/m^3), the cruising speed is u_∞ = 235.9 m/sec, the Mach number is M_∞ = 0.80, the relative atmospheric humidity is S_∞ = 0, and the vapor density is $\rho_{v\infty}$ = 0 kg/m^3.

In the cold secondary duct, for $r_{20} \le r \le r_2$, the gas flow rate is G_2 = 236.08 kg/sec, the gas velocity is u_2 = 301.4 m/sec, the pressure is p_2 = 25,206 N/m^2 (off-design parameter $N_2 = p_2/p_\infty$ = 1.1109), the temperature is T_2 = 225.95 K, the Mach number is M_2 = 1.0008, the air density is ρ_2 = 0.3891 kg/m^3, and the vapor density is ρ_{v2} = 0 kg/m^3. In the hot main duct, for $r_{10} \le r \le r_1$, the flow rate of the fuel is G_f = 0.3416 kg/sec, the flow rate of the gas mixture is G_1 = 18.66 kg/sec, the gas velocity is u_1 = 385.9 m/sec, the pressure is p_1 = 22,816 N/m^2 (off-design parameter $N_1 = p_1/p_\infty$ = 1.0056), the temperature is T_1 = 575.98 K (air density ρ_1 = 0.138 kg/m^3), the Mach number is M_1 = 0.8026, the flow rate of the vapor G_{v1} = 0.0681 kg/sec, and the vapor density is ρ_{v1} = 0.00316 kg/m^3 (relative mass concentration $Y_{v1} = \rho_{v1}/\rho_1$ = 0.0229).

The computational domain represents a rectangle of the following dimensions: r from 0 to 6.265 m and x from −2.475 to 100 m — with the FGHA′A cut corresponding to the center body and to the portion of the internal nozzle to the exit section and with a baffle separating the external flow from the external nozzle (Fig. 1).

The origin of the axial coordinate is on the exit section of the external nozzle. The domain is subdivided into nearly 86,000 cells. About 60 nodes are counted on the radius in the first duct and 90 nodes are counted in the second duct with crowding toward the walls. We set the following boundary conditions for the parameters of the gas: on portion AB, the pressure and the stagnation temperature are $p_0 = p_{02}$ = 47,760 Pa and $T_0 = T_{02}$ = 271.1 K; the direction of velocity coincides with the x axis. On portion BC, the longitudinal and transverse velocity components are $u = u_\infty$ = 235.9 m/sec and $w = w_\infty = 0$; $T = T_\infty$ = 216.7 K. On portions CD and DE, the pressure is $p = p_\infty$ = 22,690 Pa. On portion GH, the pressure and the stagnation temperature are $p_0 = p_{01}$ = 34,867 Pa and $T_0 = T_{01}$ = 659 K; the direction of velocity smoothly changes from the direction tangential to the outer wall of the nozzle to that tangential to the surface of the center body.

The boundary portions FG and HA and the baffle between the external jet and the ambient air represent impermeable adiabatic walls. The boundary condition for the tangential velocity component is set using the widespread approach, i.e., the so-called "wall law" relating the tangential stress on the wall τ_{wall} to the tangential velocity $u_{\tau 1}$ in the computational cell next to the wall:

$$\frac{u_{\tau 1}}{u_\tau} = \min\left[y_1, \ln(9y_1)/0.42\right], \quad u_\tau = \sqrt{\frac{\tau_{wall}}{\rho}}, \quad y_1 = y\frac{C_\mu^{1/4}k^{1/2}}{\mu}. \tag{15}$$

It is assumed that turbulent pulsations in the incident flow have an intensity of 0.01% and a scale of 0.1 m; the corresponding parameters in the internal jet are equal to 0.5% and 0.01 m and those in the external jet are equal to 0.2% and 0.1 m. The concentration of the steam at the inlet of the internal jet is Y_1 = 0.0229; at all the remaining boundaries, it is $Y = 0$. The problem is solved by the nonstationary method (of establishment).

Formulation of the Problem within the Framework of the Prandtl Equations. The isobaric axisymmetric jet is described by the following system [9–12]:

$$p \approx p_\infty, \quad \rho = p_\infty m/RT, \tag{16}$$

$$\rho u\frac{\partial \nu_t}{\partial x} + \rho w\frac{\partial \nu_t}{\partial r} = \frac{1}{r}\frac{\partial}{\partial r}\left\{2r\mu_t\frac{\partial \nu_t}{\partial r}\right\} + \alpha\mu_t\left|\frac{\partial u}{\partial r}\right|, \quad \mu_t = \rho\nu_t, \quad \alpha = \text{const}, \tag{17}$$

$$\frac{\partial \rho ur}{\partial x} + \frac{\partial \rho wr}{\partial r} = 0, \tag{18}$$

$$\frac{\partial \rho u^2}{\partial x} + \frac{1}{r}\frac{\partial \rho uwr}{\partial r} = \frac{1}{r}\frac{\partial}{\partial r}\left\{ r\mu_t \frac{\partial u}{\partial r} \right\}, \tag{19}$$

$$\frac{\partial \rho uH}{\partial x} + \frac{1}{r}\frac{\partial \rho wrH}{\partial r} = \frac{1}{r}\frac{\partial}{\partial r}\left\{ \frac{r\mu_t}{\mathrm{Pr}_t}\frac{\partial H}{\partial r} \right\} + \frac{1}{r}\frac{\partial}{\partial r}\left\{ r\mu_t \left(1 - \frac{1}{\mathrm{Pr}_t}\right) u \frac{\partial u}{\partial r} \right\}, \tag{20}$$

$$\frac{\partial \rho uY}{\partial x} + \frac{1}{r}\frac{\partial \rho wrY}{\partial r} = \frac{1}{r}\frac{\partial}{\partial r}\left\{ \frac{r\mu_t}{\mathrm{Sc}_t}\frac{\partial Y}{\partial r} \right\}. \tag{21}$$

In the case of a nonisobaric jet, one traditionally selects the pressure-equalization cross section with an atmospheric $p_e \approx p_\infty$ as the initial cross section and finds the temperature T_{a1} and T_{a2}, the velocity u_{a1} and u_{a2}, the mixture density ρ_{a1} and ρ_{a2}, the vapor density $\rho_{v,a1}$ and $\rho_{v,a2}$, and the transverse dimensions of the filaments (tubes) of current of the secondary and main ducts r_{a1} and $r_{a2} \equiv r_a$ from the integrals of conservation of the mixture mass and the vapor mass and the total enthalpy and entropy (as has already been noted in the Introduction):

$$G_i = \pi (r_i^2 - r_{i0}^2)\, \rho_i u_i \approx \pi r_{ai}^2 \rho_{ai} u_{ai}\,, \quad \frac{p_i}{\rho_i^\gamma} \approx \frac{p_\infty}{\rho_{ai}^\gamma}, \quad \frac{\rho_i R T_i}{m p_i} \approx \frac{\rho_{ia} R T_{ia}}{m p_\infty}, \quad i = 1, 2\,;$$

$$H_i = C_p T_i + \frac{u_i^2}{2} \approx C_p T_{ai} + \frac{u_{ai}^2}{2}, \quad G_{vi} = \pi (r_i^2 - r_{i0}^2)\, \rho_{vi} u_i \approx \pi r_{ai}^2 \rho_{v,ai} u_{ai}\,.$$

On the scale of the total jet length, we can disregard the distance to the pressure-equalization cross section; calculation begins from the nozzle exit section. Such an approach holds true within the framework of the quasi-one-dimensional approximation of flow in the tubes of current. The correspondence of the initial data for the jet can be improved by introducing corrections for the angles of deflection of the flow. We can take $x \approx l_1 + l_2$ as the pressure-equalization cross section $x = x_e$. Next, using the dual-duct engine in question as an example, we show that, with an error of several percent (for the parameters in the long-range field), we can use the resulting initial data when the angles of deflection of the surfaces shifted forward on the portions l_1 and l_2 are not small (they are 0.21 and 0.292 rad, or 12^o and 16.7^o, in the example in question). Clearly, if knowledge of the exact values of the parameters of the jet in the near-range field is required, we must use the solutions of the Navier–Stokes equations described in the previous section.

Initial and boundary conditions of system (16)–(21) have the form

$$0 \le r < r_{a1}: \quad u = u_{a1}, \quad w = 0, \quad H = H_{a1} \equiv C_p T_{a1} + \frac{u_{a1}^2}{2}, \quad \nu_t = 0.001\nu_{a1}, \quad Y = Y_a\,; \tag{22}$$

$$\nu_t (x_1, r_{a1}) = \nu_{a1} \equiv C_{\nu 1} r_{a1} \left| u_{a1} - u_{a2} \right|\,; \quad \nu_t (x_1, r = 0) = \nu_{a0} \equiv C_{\nu 1} r_{a1} u_{a1}\,; \tag{23}$$

$$r_{a1} \le r < r_a: \quad u = u_{a2}, \quad w = 0, \quad H = H_{a2} \equiv C_p T_{a2} + \frac{u_{a2}^2}{2}, \quad \nu_t = 0.001\nu_a, \quad Y = Y_\infty\,; \tag{24}$$

$$\nu_t (x_1, r_a) = \nu_a \equiv C_{\nu 2} r_a \left| u_{a2} - u_\infty \right|\,; \tag{25}$$

$$r_a \le r \le r_m: \quad u = u_\infty, \quad w = 0, \quad H = H_\infty \equiv C_p T_\infty + \frac{u_\infty^2}{2}, \quad \nu_t = 0.001\nu_a, \quad Y = Y_\infty\,; \tag{26}$$

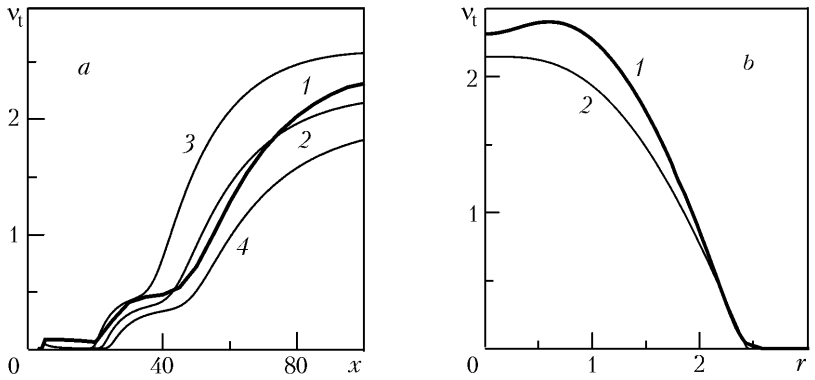

Fig. 2. Distributions of the coefficient of turbulent kinematic viscosity from the Navier–Stokes (1) and Prandtl equations (2–4) along the jet axis x (a) [2) α = 0.17; 3) 0.2; 4) 0.15] and across the jet for x = 100 m and α = 0.17 (b). ν, m^2/sec; r, x, m.

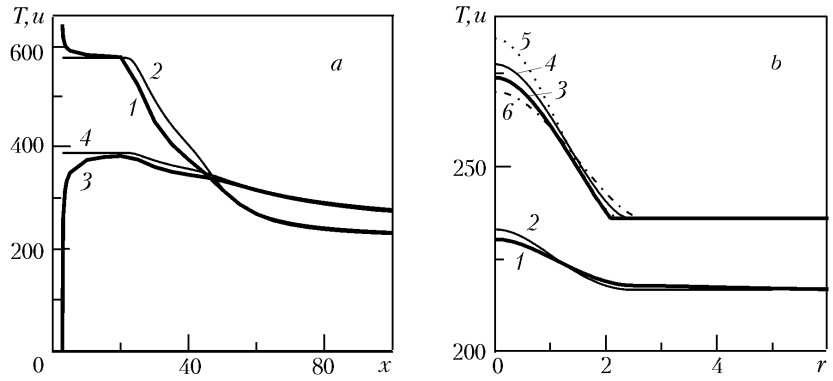

Fig. 3. Changes in the temperature T (1, 2) and the velocity u (3, 4): a) along the jet axis: 1, 3) from the Navier–Stokes equations; 2, 4) from the Prandtl equations; b) across the jet $T(r)$ (1, 2) and $u(r)$ (3–6) in the cross section x = 100 m; 1, 3) from the Navier–Stokes equations; 2, 4) from the Prandtl equations for α = 0.17; 5) α = 0.15; 6) α = 0.2. T, K; u, m/sec; r, m.

for $x_1 \cong l_2 + l_1$ and

$$\frac{\partial \nu_t}{\partial r} = 0\,, \quad \frac{\partial u}{\partial r} = 0\,, \quad w = 0\,, \quad \frac{\partial H}{\partial r} = 0\,, \quad \frac{\partial Y}{\partial r} = 0\,. \tag{27}$$

for r = 0, $r = r_m$, and $x_1 \le x \le x_m$. Here u_{a1} = 388.3 m/sec, T_{a1} = 575.07 K, and ρ_{v1} = 0.0031491 kg/m^3 are the velocity, temperature, and density of the vapor in the main duct of radius r_{a1} = 0.3334 (they have been computed from the integrals of conservation) and u_{a2} = 323 m/sec and T_{a2} = 219.3 K are the velocity and temperature in the secondary duct of radius r_a = 0.8694 m. The constants C_{v1} and C_{v2} have values close to 0.014. The turbulent viscosity has been calculated using the Kovasznay–Sekundov one-parameter model (17) with one differential equation [9–11].

Let us refer the density ρ, the velocity components u and w, and the enthalpy H to the parameters in the cocurrent flow ρ_∞, u_∞, and H_∞, the coordinates x, r to r_a, and the coefficients of turbulent dynamic viscosity μ, thermal conductivity λ, and diffusion D to the characteristic values of $\mu_a = \rho_\infty \nu_a$, $\lambda_a = C_p \mu_a / \mathrm{Pr_t}$, and $D_a = \nu_a / \mathrm{Sc_t}$. The turbulent Prandtl $\mathrm{Pr_t}$ and Schmidt $\mathrm{Sc_t}$ numbers are usually close to unity, the Reynolds number is $\mathrm{Re} = 1/(0.014 \left|1 - 1/s_2\right|)$, the Péclet number is $\mathrm{Pe} = \mathrm{Re\ Pr_t}$, and the adiabatic constant is $\gamma = C_p / C_v \approx 1.4$. The Mach number $\mathrm{M}_\infty = u_\infty / \sqrt{\gamma p_\infty / \rho_\infty}$ drops out of the energy equation for $\mathrm{Pr_t} = 1$. For $\mathrm{Pr_t}$ numbers close to unity, e.g., $\mathrm{Pr_t}$ = 0.9, the

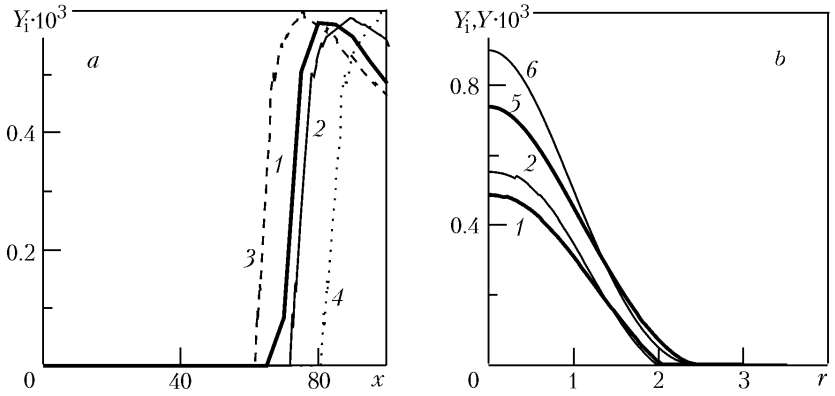

Fig. 4. Dependences of the concentration of the vapor and the condensate (ice): a) $Y_i(x)$ along the jet axis and $r = 0$: 1) according to the Navier–Stokes equations; 2) according to the Prandtl equations, $\alpha = 0.17$; 3) $\alpha = 0.2$; 4) $\alpha = 0.15$; b) across the jet $Y_i(x)$ (1, 2) and $Y(r)$ (5, 6) in the cross section $x = 100$ m, 1, 5) according to the Navier–Stokes, 2, 6) according to Prandtl, $\alpha = 0.17$.

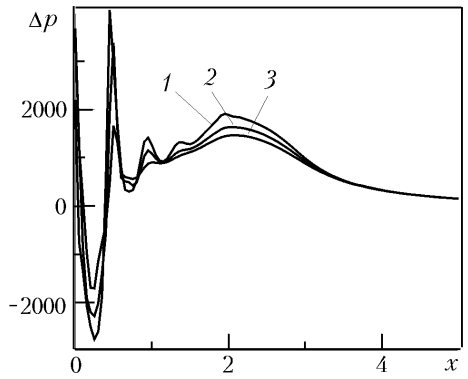

Fig. 5. Change in the pressure $\Delta p = p(x, r) - p_\infty$ along the coordinate x: 1) $r = 0.85$, 2) 0.95, and 3) 1.05 m; Navier–Stokes equations. Δp, Pa.

influence of the M number is small, too. The similarity parameters are the cocurrencies of the internal $1/s_1 = u_\infty/u_{a1}$ and external $1/s_2 = u_\infty/u_{a2}$ flows, the parameters of heating $h_1 = H_{a1}/H_\infty$ and $h_2 = H_{a2}/H_\infty$, and the relative mass concentration of the vapor on the nozzle exit section Y_a and in the atmosphere Y_∞. The Reynolds number $\mathrm{Re} = u_\infty r_a/\nu_a$ is expressed by the cocurrency $1/s_2 = u_\infty/u_{a2}$ of the secondary duct.

The solution of the problem formulated will be obtained numerically using the implicit finite-difference scheme of second order of accuracy [13, 14].

Figure 2a plots the coefficients of turbulent kinematic viscosity ν_t as functions of the coordinate x for different values of the coefficient α (0.2, 0.17, and 0.15) in the source term of the Kovasznay–Sekundov equation (17). Satisfactory agreement with the results of calculation of the Navier–Stokes equations (curve 1) has been obtained for $\alpha = 0.17$ (curve 2). Figure 2b plots the transverse distributions of the coefficient of turbulent kinematic viscosity $\nu_t(r)$, which have been obtained from the Navier–Stokes equations (curve 1) and the Prandtl equations in the present section for $\alpha = 0.17$ (curve 2). We note a satisfactory agreement of the transverse dimensions of the jet in viscosity in both models.

The remaining parameters of the jet — temperature, velocity, and concentrations of the vapor and the condensate — satisfactorily coincide in both the longitudinal direction along the x axis (Figs. 3a and 4a) and the transverse direction (Figs. 3b and 4b), too. Pressure is rapidly equalized to the atmospheric one for $x \le 5$ in both the longitudinal and transverse directions (Fig. 5). Satisfactory agreement of the solutions within the framework of (elliptic-type) Navier–Stokes and (parabolic-type) Prandtl equations has also been obtained for the concentration of any other diffus-

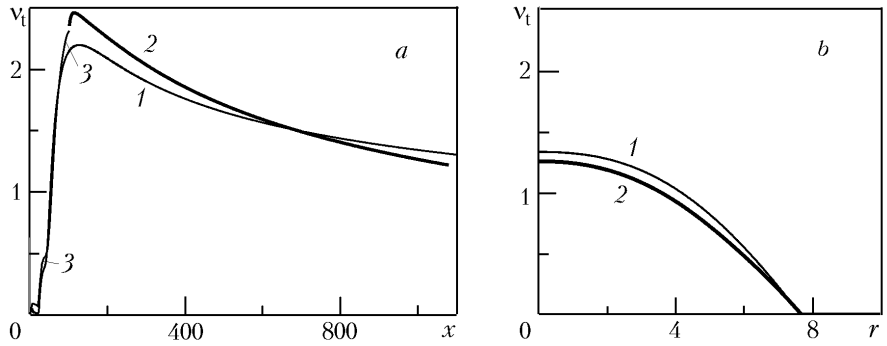

Fig. 6. Changes in the turbulent viscosity along the jet axis (a) and across the jet in the cross section x = 1000 m (b) [1) method 1; 2) method 2; 3) calculation from the Navier–Stokes equations]. ν, m^2/sec; x, r, m.

ing component, for example, carbon dioxide CO_2. Thus, results close to the solutions of the Navier–Stokes equations and differing by several percent have been obtained in the cross section x = 100 m for α = 0.17. Such differences are, admittedly, insignificant for the turbulent jet.

In actual fact, an agreement of the solutions within the framework of the Navier–Stokes and Prandtl equations with an error of several percent has been obtained in the interval $\Delta x \approx$ 10 m preceding the reference cross section x = 100 m. We note that, as will be shown below, a difference of only several percent in temperature and velocity in the long-range field has been found in two variants of conjugation of the solution domains of the Navier–Stokes and Prandtl equations for x = 100 m, and, for example, for x = 90 m. As has been mentioned above, such an accuracy is acceptable for calculation of the turbulent jet.

Long-Range Field. The solutions for the long-range field will be obtained by two methods: 1) we assign the profiles of the functions sought computed from the Navier–Stokes equations in the cross section x = 100 m as the initial ones for the Prandtl equations; 2) we continue calculation of the Prandtl equations so that the entire jet is calculated within the framework of parabolic gasdynamic equations, i.e., Prandtl equations.

Figure 6a shows changes in the coefficient of turbulent kinematic viscosity ν along the axis for r = 0 m at distances above 1 km. Figure 6b gives the corresponding transverse distributions in the cross section x = 1000 m. The differences in viscosity ν amount to about 11% at the maximum point (x = 113–115 m) and to 6% at the distance x = 1000 m.

The changes in the temperature T and the velocity u along the jet and across it in the long-range field (x = 500–1300 m), obtained for variants 1 and 2, differ insignificantly: at x = 1000 m, the differences in temperature are 0.07% and those in velocity are 0.24%.

The concentrations of the vapor $Y(x)$ and the condensate $Y_i(x)$ (ice) along the axis (r = 0) are presented in Fig. 7a; those across the axis in the cross section x = 1000 m are given in Fig. 7b and c. The differences in the quantities $Y_i(r)$ and $Y(r)$, computed by two methods, for x = 1000 m are relatively small and amount to 19 and 2.4%. Good agreement of the transverse dimensions of the jet in vapor and condensate concentrations and in velocity, temperature, and turbulent-kinematic-viscosity-coefficient distributions is noteworthy. The influence of the quantity α is shown by curves 6 and 7 in Fig. 7b.

Table 1 gives the basic characteristics (obtained by two methods) of the jet: the coordinate of collapse of the aerosol on the x^* axis, the radius of the condensation trail (contrail) in this cross section r_c^*, the coordinates x_{mY}, x_m, $x_{m\nu}$, and x_{mr} and the corresponding values of the maximum concentration of the condensate (ice) on the $Y_i(x_{mY}, r = 0) = Y_{i,m}$ axis, the maximum cross section-average concentration of the condensate $Y_{i,av}(x_m) = Y_{i,av,m}$, the maximum coefficient of kinematic viscosity $\nu_t(x_{m\nu}) = \nu_m$, the maximum radius $r_{c,m}$ of the contrail, the total length of the contrail L_c, and the final radius of the contrail r_{L_c}. The length L_c has been computed for the contrail from the level of the condensate density ρ_i in the closing part; it is equal to 1% of its maximum value $\rho_{i,m}$. The remaining part of the contrail is omitted, since it makes no contribution to the total condensate mass, in practice.

The value of the cross section-average concentration of the condensate $Y_{i,av}(x)$ is computed from the formula

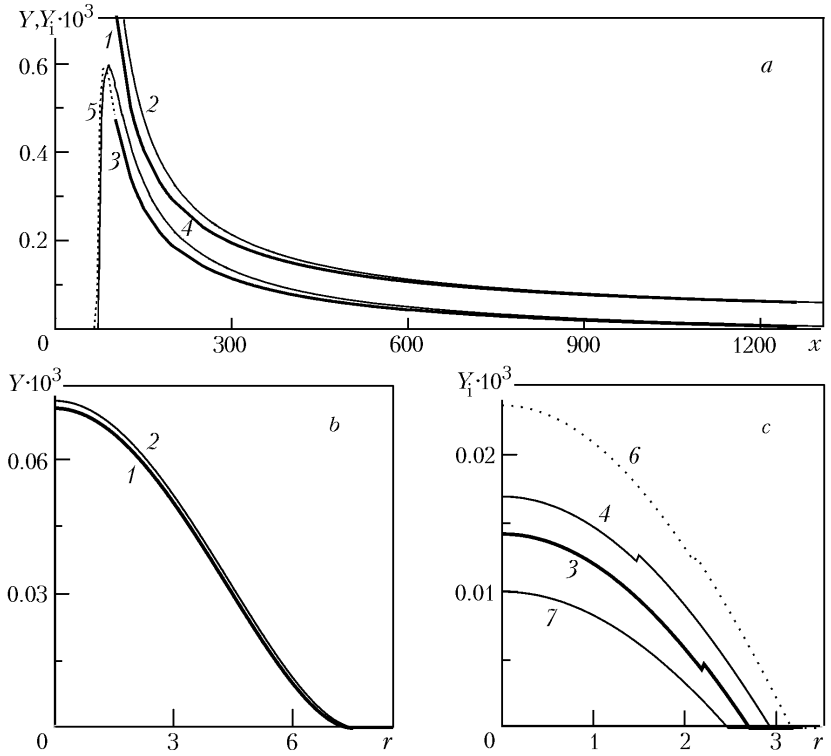

Fig. 7. Distributions of the vapor $Y(x)$ (1, 2) and condensate concentrations $Y_i(x)$ (3–7) along the jet axis (a) and across the jet in the cross section x = 1000 m (b, c): 1, 3) method 1; 2, 4) method 2 (α = 0.17); 5) calculation from the Navier–Stokes equations; 6) α = 0.15; 7) α = 0.2. r, x, m.

TABLE 1. Basic Characteristics of the Exhaust Jet, Obtained by Two Methods

Method	x^*, m	r_c^*, m	x_m, m	$Y_{i,av,m}$	x_{mY}, m	$Y_{i,m}\cdot 10^4$	$x_{m\nu}$, m	ν_m, m^2/sec	x_{mr}, m	$r_{c,m}$, m	L_c, m	r_{Lc}, m
1	70	2.01	—	—	80	5.89	114	2.46	509	3.33	1261	1.68
2	72	1.56	76.6	$2.84\cdot 10^{-4}$	78	5.02	126	2.20	551	3.45	1308	1.98

$$Y_{i,av}(x) = \frac{\int_0^{r_c} 2\pi r\,[Y(x, r) - Y_{s,i}]\,dr}{\pi r_c^2},$$

where r_c is the running radius of the contrail, and the concentration of a saturated vapor $Y_{s,i}$ above the condensate (ice) is computed from the Clausius–Clapeyron formula

$$Y_{s,i}(T) = Y_{s,i\infty} \exp\left\{\int_{T_\infty}^{T} \frac{m_w L_w dT}{RT^2}\right\}.$$

Good agreement of the jet characteristics computed for both $x > 100$ m, i.e., within the framework of the same (Prandtl) equations, and $x < 100$ m, i.e., from the Navier–Stokes and Prandtl equations, should be noted. The average-over-the-jet gasdynamic quantities to a cross section of 100 m have not been computed. The maximum radius $r_{c,m}$ and the contrail length L_c for methods 1 and 2 differ by 8.3 and 3.7% respectively.

If we compare the parameters obtained for method 2 when $\alpha = 0.17$ to the corresponding parameters of the jet that have been computed in [12] for the typical value of $\alpha = 0.2$ recommended in [1], we can note that the correction does not lead to pronounced changes in the basic physical parameters of the jet. Substantial changes will be obtained with a two-fold increase in the coefficient α, as has been shown earlier in [12].

Conclusions. In the case of violation of the conditions of quasi-one-dimensionality of flow of an exhaust jet (considerable angles of deflection of the filaments of current due to the nozzle geometry) in the near-range field we must solve elliptic-type equations (Navier–Stokes equations or in this case their analog — Reynolds equations for the average turbulent parameters) to determine the parameters of the jet. The low nonisobaricity and the conditions of sticking and turbulization in the boundary layers and mixing layers (main and secondary ducts in the case of a dual-duct engine) are allowed for. The long-range field must be calculated using parabolic-type equations. Also, we can allow for the influence of the real geometry of the structure of the exhaust nozzle of an aircraft engine in calculating both the near-range and long-range fields of the jet within the framework of parabolic-type equations (boundary-layer Prandtl equations) using correction of the constant in the source term for the coefficient of turbulent kinematic viscosity. Investigation of the influence of the parameters controlling the jet (average values of the temperature, velocity, and concentration of the vapor, transverse distributions of the parameters on the nozzle exit section, and increase in the coefficient of viscosity on the nozzle exit section and in the jet volume) is conveniently carried out within the framework of the Prandtl equations after the corresponding correction of the constants appearing in the turbulence model. It is desirable to perform such a correction based on experimental data, too, since the turbulence model appearing in elliptic-type equations (Navier–Stokes ones) in turn contains empirical auxiliary functions and constant coefficients. The range of validity of any of the turbulence models existing at present is bounded by the corresponding temperature, velocity, and condensation ranges in which the auxiliary functions and constant quantities have been obtained.

This work was carried out with support from the leading scientific schools, grant NSh-1984.2003.1.

NOTATION

C_p and C_v, specific heats at constant pressure and volume, J/(kg·K); C_μ, C_{v1}, and C_{v2}, numerical coefficients; D, diffusion coefficient, m^2/sec; G, mass flow rate, kg/sec; h_1 and h_2, parameters of heating; H, total enthalpy of the gas, J/kg; j_j, components of the diffusion-vapor-flow vector, kg/(m^2·sec); k, kinetic turbulence energy, m^2/sec; L_w, specific heat of condensation, J/kg; l, distance along the jet axis, m; L_c, condensation-trail (contrail) length, m; m and m_w, molar mass of the mixture of a gas and a steam; M, Mach number; p, gas pressure, Pa; Pr, Prandtl number; Pe, Péclet number; q_j, components of the heat-flux vector, W/m^2; r, radial coordinates, m; r_{10}, r_1 and r_{20}, r_2, radii of the internal and external contours of the nozzle, m; r_{a1} and $r_{a2} = r_a$, radii of the tubes of current from the internal and external contours of the nozzle in the pressure-equalization cross section, m; r_c, contrail radius, m; r_c^*, radius of the contrail in the cross section of collapse of the aerosol on the axis, m; $r_{c,m}$, maximum radius of the contrail, m; r_{L_c}, final radius of the contrail (in the cross section $x = L_c$), m; R, universal gas constant, J/(mole·K); Re, Reynolds number; x, coordinate along the jet axis, m; s_{ij}, components of the strain-rate tensor, sec^{-1}; $1/s_1$ and $1/s_2$, parameters of cocurrency of the internal and external flows; S_∞, relative atmospheric humidity; Sc, Schmidt number; t, time, sec; T, gas temperature, K; u_i, u_j, and u_k (i, j, and k = 1, 2, and 3), components of the gas velocity, m/sec; u and w, velocity components, m/sec; u_τ, characteristic velocity in the boundary layer, m/sec; $u_{\tau 1}$, velocity in the grid node next to the surface, m/sec; x_i, x_j, and x_k (i, j, and k = 1, 2, and 3), Cartesian coordinates, m; x^*, distance to the cross section of collapse of the aerosol on the axis, m; x_m, cross section in which the value of the cross section-average concentration of the condensate is maximum, m; x_{mY}, cross section of the maximum concentration of ice on the axis, m; $x_{m\nu}$, cross section of the maximum coefficient of viscosity, m; x_{mr}, coordinate of the maximum radius of the contrail, m; y_1, dimensionless distance from the surface to the grid node next to it; Y and Y_i, relative mass concentrations of the vapor and the condensate (ice); $Y_{s,i\infty}$, concentration of the vapor saturated above ice; $Y_{i,m}$, maximum concentration of the condensate (ice) on the axis; $Y_{i,av}$, cross section-average concentration of the condensate; $Y_{i,av,m}$, maximum cross section-average concentration of the condensate; α, numerical coefficient; γ, adiabatic exponent; δ_{ij}, Kronecker symbol; ε, rate of dissipation of kinetic turbulence energy, m^2/sec^3; η, dimensionless parameter of the turbulence model; λ, thermal-conductivity coefficient, W/(m·K); μ, coefficient of dynamic viscosity, Pa·sec; ν, coefficient of kinematic viscosity, m^2/sec; ρ, gas density, kg/m^3; ρ_i, condensate (ice) density, kg/m^3; $\rho_{i,m}$, maximum condensate density, kg/m^3; σ_k and

σ_ε, dimensionless parameters of the turbulence model; τ_{ij}, components of the stress tensor, N/m^2; τ_{wall}, friction stress on the surface, N/m^2. Subscripts: a, initial average parameters of the jet in the pressure-equalization cross section (they are referred to the nozzle exit section); av, running average parameters; c, contrail; e, equilibrium, referring to the cross section of equalization of pressure to the atmospheric one; f, fuel; i and j = 1, 2, and 3, vector or tensor components; i, ice; m, maximum; s, saturated; t, turbulent; v, vapor (steam); w, water; wall, wall; ∞, at a large distance in an unperturbed gas; 0, initial cross section; 1 and 2, main and secondary ducts (internal and external contours); *, coordinate of collapse of the aerosol on the axis.

REFERENCES

1. G. N. Abramovich, T. A. Girshovich, S. Yu. Krasheninnikov, et al., *Theory of Turbulent Jets* [in Russian], Nauka, Moscow (1984).
2. G. N. Abramovich, *Applied Gas Dynamics* [in Russian], Pt. 1, Nauka, Moscow (1991).
3. V. E. Kozlov, A. N. Sekundov, and I. P. Smirnova, Axisymmetric turbulent compressed jet in a subsonic cocurrent flow, in: V. V. Struminskii (Ed.), *Problems of Turbulent Flows* [in Russian], Nauka, Moscow (1987), pp. 171–177.
4. A. N. Kucherov and G. V. Molleson, Condensation wake in a nonisobaric jet, *Inzh.-Fiz. Zh.*, **74**, No. 5, 29–32 (2001).
5 A. V. Kashevarov, A. N. Kucherov, and G. V. Molleson, Dependence of the optical characteristics of the condensation trail on the laws of distribution of the parameters of a nonisobaric exhaust jet at the nozzle cut exit section, *Opt. Atmos. Okeana*, **14**, No. 5, 418–423 (2001).
6. *Aviation. Encyclopedia* [in Russian], BES, Moscow (1994).
7. L. G. Loitsyanskii, *Mechanics of Liquids and Gases* [in Russian], Nauka, Moscow (1973).
8. V. Yakhot, S. A. Orszag, S. Tangam, T. B. Gatski, and C. G. Speziale, Development of turbulence models for shear flows by a double expansion technique, *Phys. Fluids*, **A4**, No. 7, 1510–1520 (1992).
9. L. S. G. Kovasznay, Structure of the turbulent boundary layer, *Phys. Fluids.*, **10**, No. 9, Pt. 2, 25–30 (1967).
10. V. M. Nee and L. S. G. Kovasznay, Simple phenomenological theory of turbulent shear flows, *Phys. Fluids*, **12**, No. 3, 473–484 (1969).
11. A. N. Sekundov, Application of the differential equation for eddy viscosity to analysis of plane self-similar flows, *Izv. Akad. Nauk SSSR*, *Mekh. Zhidk. Gaza*, No. 5, 114–127 (1971).
12. A. N. Kucherov, Control of the parameters of an exhaust jet by increasing the eddy viscosity of the nozzle edge, *Inzh.-Fiz. Zh.*, **76**, No. 6, 29–37 (2003).
13. V. A. Ruskol and U. G. Pirumov, An isobaric turbulent reacting jet escaping to a cocurrent flow, *Dokl. Akad. Nauk SSSR*, **236**, No. 2, 321–324 (1977).
14. V. S. Avduevskii, D. A. Ashratov, A. V. Ivanov, and U. G. Pirumov, *Supersonic Nonisobaric Gas Jets* [in Russian], Mashinostroenie, Moscow (1985).